arXiv:1511.00408v2 [physics.optics] 5 Jan 2016

# TE resonances in graphene-dielectric structures

**J. F. M. Werra[1], F. Intravaia[2] and K Busch[1,2]**

[1] Humboldt-Universität zu Berlin, Institut für Physik, AG Theoretische Optik & Photonik, 12489 Berlin, Germany

[2] Max Born Institute, 12489 Berlin, Germany

E-mail: jwerra@physik.hu-berlin.de

**Abstract.** We investigate the dispersion relations of TE resonances in different graphene-dielectric structures. Previous work has shown that when a graphene layer is brought into contact with a dielectric material, a gap can appear in its electric band structure. This allows for the formation of TE-plasmons with unusual dispersion relations. In addition, if the dielectric has a finite thickness, graphene strongly modifies the behavior of the waveguiding modes by introducing dissipation above a well-defined cutoff frequency thus providing the possibility of mode filtering. This cutoff and the properties of TE-plasmons are closely related to the pair-creation threshold of graphene thus representing quantum mechanical effects that manifest themselves in the electromagnetic response.

PACS numbers: 68.65.Pq, 71.45.Gm, 73.20.Mf, 78.67.Wj

## 1. Introduction

The physics of graphene is often described in terms of a (2 + 1)-dimensional Dirac field where the speed of light is replaced by the Fermi velocity, $v_{\rm F}$. For pristine graphene in vacuum the effective Dirac field is massless and the resulting energy band structure near the Fermi level is characterized by the very well know linear dispersion relation (Dirac cone) associated with the K-points at the corners of the Brilloin zone [1]. Previous work has shown, however, that in certain circumstances graphene's band structure can feature an electronic band gap $2\Delta$ ($\Delta \approx 5 - 50\,\mathrm{meV}$ [2, 3, 4], see Fig. 1) which can be modeled as an effective mass in the Dirac model. This effective mass can be related to the occurrence of one or several physical phenomena, such as the presence of impurities, the contact with another medium (i.e., substrate), strain, etc. The modified electronic band structure affects the optical response of graphene and, specifically, also its peculiar plasmonic resonances. These interesting features are attracting growing attention as witnessed by the vast number of recent publications addressing their properties (for instance, see Refs. [5, 6, 7, 8, 9, 10]). In contrast to other two-dimensional electron gases that only exhibit "ordinary" TM-polarized plasmon resonances, graphene also exhibits a resonant response to TE-polarized light [11]. When utilizing a gapless model, it turns out that while TE-plasmons remain when graphene is embedded into a dielectric material, they disappear when graphene is sandwiched between two different dielectrics [12, 13]. However, when graphene is deposited on a substrate (e.g., hexagon boron-nitride or silicon carbite), the offset in lattice spacing between the two materials can lead to the opening of a relatively wide band gap [2, 3, 4, 14], rendering a gapless description inadequate. In this work, we investigate the existence of TE plasmons for certain prototypical graphene-dielectric configurations, introducing the gap as phenomenological parameter on the order of tens of meV (see, for instance, the ab-initio study [4]). We demonstrate how the appearance of a band gap and the pair-creation threshold affect the dispersion relations of the TE resonances, conferring distinct quantum feature upon them.

## 2. Resonances in graphene-dielectric systems

In the following, we employ dimensionless units such that velocities are expressed in units of the vacuum speed of light $c$ and frequencies are measured in units of the band gap $2\Delta/\hbar$. This amounts to the replacements $v_{\rm F}/c \to v_{\rm F}$ and $\hbar\omega/(2\Delta) \to \omega$, respectively, and the in-plane wavevector changes accordingly $\hbar ck/(2\Delta) \to k$. Following the quantum-field theoretical description of graphene discussed in earlier works [15, 16, 17, 18], we relate its optical properties to two components of the polarization tensor

$$\Pi_{00} = \alpha \frac{k^2}{v_{\rm F}^2 k^2 - \omega^2} \Phi(\omega, k)\,, \quad \Pi_{\rm tr} = \alpha \frac{(v_{\rm F}^2 + 1)k^2 - 2\omega^2}{v_{\rm F}^2 k^2 - \omega^2} \Phi(\omega, k), \tag{1}$$

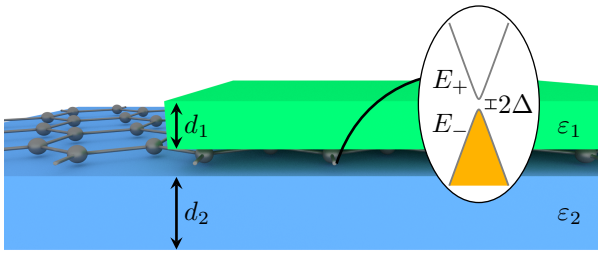


**Figure 1.** Schematics of the graphene-dielectric structure considered in this work. The inset depicts the electronic band structure of graphene in the vicinity of the Dirac cone $E_\pm = \pm\sqrt{\Delta^2 + \hbar^2 v_\mathrm{F}^2 k^2}$. Here, the in-plane wavevector $k$ is measured from the K-points of the Brillouin zone and $v_\mathrm{F}$ denotes the Fermi velocity.

where we have introduced $\Phi(\omega, k) \equiv \Phi(y) = 2\left[1 - \frac{y^2+1}{y^2} y \operatorname{arctanh}(y)\right]$ with $y = \sqrt{\omega^2 - v_\mathrm{F}^2 k^2}$ and $\alpha = 137^{-1}$ denotes the fine structure constant. Using these quantities, the electromagnetic reflection and transmission coefficients for a single and freely suspended graphene layer are given by [15, 16]

$$r_g^{\mathrm{TM}} = \frac{\kappa_0 \Pi_{00}}{k^2 \Pi_{\mathrm{tr}} - \kappa_0^2 \Pi_{00} + 2k^2 \kappa_0}\,, \qquad t_g^{\mathrm{TM}} = 1 - r_g^{\mathrm{TM}}\,, \tag{2}$$

$$r_g^{\mathrm{TE}} = \frac{k^2 \Pi_{\mathrm{tr}} - \kappa_0^2 \Pi_{00}}{\kappa_0 \Pi_{00} + 2k^2}\,, \qquad t_g^{\mathrm{TE}} = 1 + r_g^{\mathrm{TE}}\,. \tag{3}$$

Here, we have defined $\kappa_0 = \sqrt{k^2 - \omega^2} \equiv -\mathrm{i}k_0^\perp$, which is related to the vacuum wavevector component $k_0^\perp$ orthogonal to the plane of the graphene layer. When a single graphene layer is embedded between two slabs made of different dielectric materials and/or different thicknesses (cf. Fig. 1), the reflection and transmission coefficients can be found using the transfer matrix technique [19, 20]

$$\mathcal{T} = \mathcal{T}_2 \cdot \mathcal{T}_{\mathrm{graphene}} \cdot \mathcal{T}_1\,, \qquad \text{where } \mathcal{T}_i = \frac{1}{t_i}\begin{pmatrix} t_i^2 - r_i^2 & r_i \\ -r_i & 1 \end{pmatrix}. \tag{4}$$

The expression of $\mathcal{T}_i$ is characteristic for a homogeneous dielectric layer [21] where $r_i$ and $t_i$, respectively, represent the layer's reflection and transmission coefficients. From a straightforward calculation for illumination from the side of layer 1, we obtain that the scattering properties of the multilayer structure are described by

$$r = r_1 + t_1^2 \frac{r_g + r_2\left(t_g^2 - r_g^2\right)}{(r_2 r_g - 1)(r_1 r_g - 1) - r_1 r_2 t_g^2}\,, \tag{5}$$

$$t = \frac{t_1 t_g t_2}{(r_2 r_g - 1)(r_1 r_g - 1) - r_1 r_2 t_g^2}\,. \tag{6}$$

While for the reflection and transmission coefficients of graphene, $r_g$ an $t_g$, we can utilze Eqs. (2) and (3), the dielectric layers' scattering coefficients, $r_i$ and $t_i$, depend on the thickness $d_i$ and on the material permittivity $\varepsilon_i$. For the case of TE polarized radiation

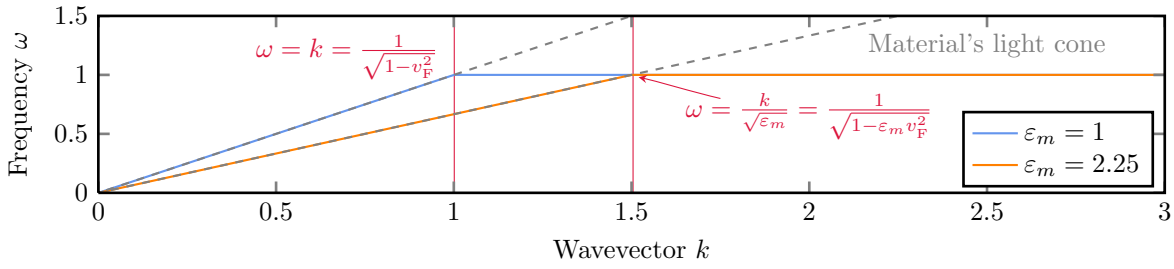


**Figure 2.** Dispersion relation of the TE plasmon for a freely suspended graphene layer ($\varepsilon_m = 1$) and when embedded in an infinite dielectric with permittivity $\varepsilon_m = 2.25$.

and considering the total structure with vacuum on both sides we explicitly obtain

$$r_i = \frac{\left(\frac{\kappa_0-\kappa_{m,i}}{\kappa_0+\kappa_{m,i}}\right)\left(1-\mathrm{e}^{-2d_i\kappa_{m,i}}\right)}{1-\left(\frac{\kappa_0-\kappa_{m,i}}{\kappa_0+\kappa_{m,i}}\right)^2\mathrm{e}^{-2d_i\kappa_{m,i}}}, \qquad t_i = \frac{\left[1-\left(\frac{\kappa_0-\kappa_{m,i}}{\kappa_0+\kappa_{m,i}}\right)^2\right]\mathrm{e}^{-d_i\kappa_{m,i}}}{1-\left(\frac{\kappa_0-\kappa_{m,i}}{\kappa_0+\kappa_{m,i}}\right)^2\mathrm{e}^{-2d_i\kappa_{m,i}}}, \tag{7}$$

where $\kappa_{m,i} = \sqrt{k^2 - \varepsilon_i\omega^2}$ and $i = 1, 2$. Anticipating that we will investigate phenomena in the low THz regime, we approximate the material permittivities by their static value. Further, in our dimensionless units, the slabs' thicknesses $d_i$ undergo the replacement $2\Delta d_i/\hbar c \to d_i$.

The above expressions describe several different setups where graphene is combined with a dielectric environment and in the following we focus on four specific configurations: First, we investigate a setup where a single graphene layer is embedded in an infinitely thick dielectric material ($d_i \to \infty$, $\varepsilon_i \equiv \varepsilon_m$). Then, we consider the case of a where a graphene layer is placed between two identical dielectric slabs with finite thickness ($d_i = d$, $\varepsilon_i \equiv \varepsilon_m$). Next, we generalize the above "sandwich" configuration to an asymmetric setup where a graphene layer is deposited first on an infinite dielectric substrate ($d_1 \to \infty$, $d_2 \to \infty$, $\varepsilon_1 = 1$, $\varepsilon_2 \equiv \varepsilon_m$) and, finally, we consider a graphene layer on a dielectric slab with finite thickness ($d_1 \to \infty$, $d_2 \equiv d$). For all configurations we will determine the structures' resonances in the response to TE-polarized electromagnetic radiation. Mathematically, this corresponds to investigating the condition

$$\frac{1}{r} = 0 \qquad \Leftrightarrow \qquad (r_1 r_g - 1)(r_2 r_g - 1) = r_1 r_2 t_g^2 \,. \tag{8}$$

This provides the starting point of all analyses in the subsequent sections.

## 3. Graphene embedded in an infinitely extended dielectric

When a graphene layer is embedded in an infinitely extended dielectric Eq. (8) is equivalent to $\alpha\Phi(y) + 2\kappa_m = 0$. For freely suspended graphene ($\varepsilon_m = 1$), the numerical solutions of this equation have already been analyzed in Ref. [17, 18]. Here, we rather present the dispersion relation in terms of a parametric expression. Setting $y = \tanh(q)$,

where $q$ is the external parameter, we obtain that the TE resonance is described by

$$k[q] = \frac{1}{\sqrt{1-\varepsilon_m v_{\rm F}^2}} \sqrt{\varepsilon_m \tanh(q)^2 + \alpha^2 \left( q \frac{\tanh(q)^2+1}{\tanh(q)} - 1 \right)^2} \qquad (9a)$$

$$\omega[q] = \frac{1}{\sqrt{1-\varepsilon_m v_{\rm F}^2}} \sqrt{\tanh(q)^2 + \alpha^2 v_{\rm F}^2 \left( q \frac{\tanh(q)^2+1}{\tanh(q)} - 1 \right)^2} \,. \qquad (9b)$$

In Fig. 2, we depict the dispersion relation (9$a$), and (9$b$) for $\varepsilon_m = 2.25$ and for vacuum $\varepsilon_m = 1$. The latter curve agrees with the corresponding numerical results [17]. The complete TE-plasmon dispersion relation lies in the embedding medium's evanescent region, i.e., below the embedding medium's light cone ($\omega < k/\sqrt{\varepsilon_m}$). We can clearly distinguish two regimes: For low frequencies, $\omega < 1$ (or, equivalently, $k < \sqrt{\varepsilon_m}$), the TE-plasmon dispersion relation is close to the light cone $\omega = k/\sqrt{\varepsilon_m}$ and can be well approximated by $\omega[k] = \beta(k)\, k$, where

$$\beta(k) \approx \frac{\sqrt{1 - \frac{16}{9}\alpha^2 \left( \frac{1-\varepsilon_m v_{\rm F}^2}{\varepsilon_m} \right)^2 k^2}}{\sqrt{\varepsilon_m}} \lesssim \frac{1}{\sqrt{\varepsilon_m}}, \qquad (10)$$

For high frequencies, $\omega \gtrsim 1$ (or, equivalently $k > \sqrt{\varepsilon_m}$), the TE-plasmon dispersion relation is practically independent of the embedding dielectrics' properties ($q \gtrsim 1$)

$$k[q] \approx \sqrt{\frac{\varepsilon_m (2\tanh(q) - 1) + \alpha^2 (2q-1)^2}{1-\varepsilon_m v_{\rm F}^2}}, \qquad (11)$$

$$\omega[q] \approx \sqrt{\tanh(q)^2 + v_{\rm F}^2 k^2} \,.$$

so that for these frequencies the dispersion relation becomes very flat and takes on an almost constant value for $v_{\rm F} \ll 1$. The transition between these two rather distinct regimes of the dispersion relations occurs near $\omega \approx 1$ (or, equivalently, $k \approx \sqrt{\varepsilon_m}$). Due to the small value of the fine structure constant $\alpha$, this transition range is rather small, so that the transition appears to be rather abrupt. However, formally studying the behavior of the dispersion relation for larger values of $\alpha$, reveals that this apparent "kink" is actually a smooth crossover [17, 18]. In the following, we will utilize this formal trick of considering larger values of $\alpha$ for better representing this feature [17, 18].

## 4. A graphene layer between two identical dielectric slabs with finite thickness

The physics becomes considerably richer when a graphene layer is sandwiched between two identical dielectric slabs of finite thickness $d$. For this configuration, Eq. (8) leads to two different sets of modes. The first set is given by the solutions of

$$r_m^{\rm TE} + 1 = 0 \qquad (12)$$

which corresponds to waveguide modes with odd symmetry for a slab of thickness $d' = 2d$ (see Fig. 3). Since these modes have zero field at the position of the graphene sheet,

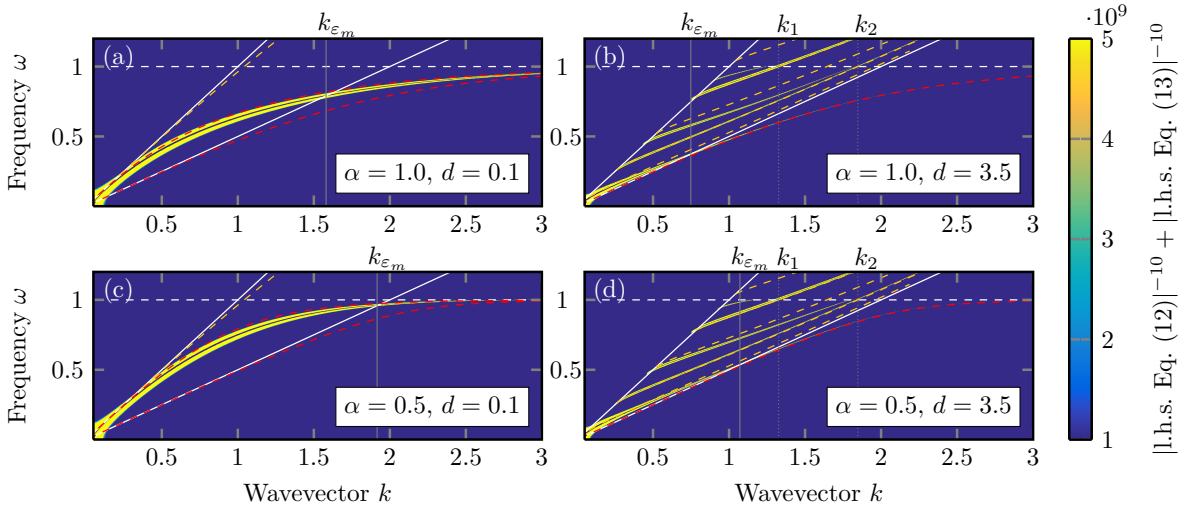


**Figure 3.** TE-plasmon resonances for a slab-graphene-slab setup with $\varepsilon_m = 4.0$ and different thickness $d$ of the dielectric slabs. For representation purposes we use values $\alpha = 1, 1/2$ which artifically enlarge the transition region [17, 18]. Color-coded is the behavior of the inverse absolute value of the l.h.s. of Eq. (13) and the equivalent for the solution $r_m^{\mathrm{TE}} = -1$. The orange dashed lines describe the modes of a single dielectric slab (with $d' = 2d$ and without graphene). The dashed red line represent the TE-plasmon resonances (see Eqs. (9*a*) and (9*b*)) for graphene suspended in vacuum (upper curve) and embedded in an infinite dielectric with $\varepsilon_m = 4.0$ (lower curve). The white solid lines represent vacuum and material light cones. The dashed line marks the pair-creation threshold with $\omega = \sqrt{1 + v_{\mathrm{F}}^2 k^2}$ (see text for further details).

they are not affected by its presence. Therefore, while we retain these unaltered modes, we concentrate in the following discussion mainly on the altered modes. Equation (8) provides, in fact, a second (the even) set of modes which are the solution of

$$\begin{aligned} &\alpha\Phi(y)\left[\kappa_0 + \kappa_m - \mathrm{e}^{-2d\kappa_m}\left(\kappa_0 - \kappa_m\right)\right] \\ &\qquad + 2\kappa_m\left[\kappa_m + \kappa_0 + \mathrm{e}^{-2d\kappa_m}\left(\kappa_0 - \kappa_m\right)\right] = 0\,. \end{aligned} \tag{13}$$

This can be rewritten in the more convenient form

$$d = \frac{1}{2\kappa_m}\ln\left[\frac{\left(\kappa_0 - \kappa_m\right)\left(\alpha\Phi(y) - 2\kappa_m\right)}{\left(\kappa_0 + \kappa_m\right)\left(\alpha\Phi(y) + 2\kappa_m\right)}\right]. \tag{14}$$

Owing to the fact that $d$ is a real number, Eq. (14) allows for real valued solutions only in certain regions of the $(k, \omega)$-plane. Indeed, when $k < \omega$ (propagating waves in vacuum) neither damped nor undamped waveguide modes exist ($d$ is always complex since $\kappa_0 - \kappa_m < 0$). Additionally, for $y > 1$ (the single particle excitation region of graphene above the pair-creation threshold), the r.h.s. of the Eq. (14) necessarily has an nonzero imaginary part and therefore only damped modes can exist (see below).

In the remaining regions, Eq. (14) exhibits two sets of physically distinct solutions. The first set of modes is located in the region $\omega < k < \omega\sqrt{\varepsilon_m}$ with $y \leqslant 1$ and corresponds to guided, real frequency modes propagating in the slab, i.e., modes that exhibit an evanescent orthogonal wavevector in vacuum. The existence of these solutions can be understood by noticing that in this region $k_m^{\perp} = \mathrm{i}\kappa_m$ and $-\alpha\Phi(y)$ are positive numbers.

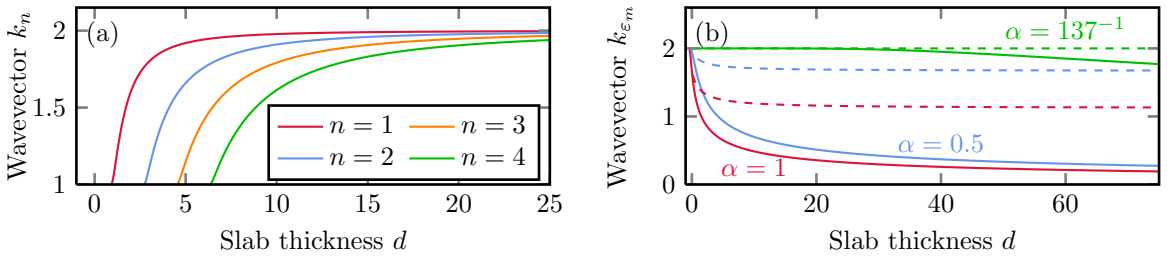


**Figure 4.** Panel (a): Thickness dependence of the cutoff wavevectors $k_n[d]$ for $n = 1, 2, 3, 4$ that determine the behavior of waveguiding in graphene-dielectric-slab systems. Panel (b): Thickness dependence of the wavevector for which the TE-plasmon resonance crosses the dielectric material's light cone. We consider different values of $\alpha$ and show the results for graphene on a slab (dashed) and graphene between two slabs (solid) in order to connect to the results of Figs. 3 and 7. See text for further details.

Upon rewriting Eq. (14) we, therefore, obtain

$$d = \frac{\arctan\left(\frac{2k_m^\perp}{-\alpha\Phi(y)}\right) - \arctan\left(\frac{2k_m^\perp}{2\kappa_0}\right) + \pi n}{k_m^\perp} > 0, \tag{15}$$

where $n = 1, 2, 3, \ldots$ (see below for the case $n = 0$). Each value of $n$ corresponds to a different waveguide mode. Interestingly and in contrast to ordinary guided modes in a dielectric slab, the incorporation of a graphene layer sets a cutoff to the dispersion relations for these lossless modes on the line $y = 1$. We display these modes – together with the undisturbed, odd modes ($r_m^{\mathrm{TE}} = -1$) – in Fig. 3 where, for clarity of the presentation, we have used values $\alpha = 1,\ 1/2$ for the fine structure constant. The actual values of the cutoff wavevectors $k_n$, for which the waveguide modes cross the cutoff line, depend on the value of $n$, on the dielectric function and the thickness of the slab. For each $n$ the function $k_n[d]$ can be described in terms of the following parametrization

$$d[k_m^\perp] = \frac{2\pi n - \arctan\left(\frac{\sqrt{1-\varepsilon_m v_{\mathrm{F}}^2}\,k_m^\perp}{\sqrt{(\varepsilon_m - 1) - \left(1-\varepsilon_m v_{\mathrm{F}}^2\right)\left(k_m^\perp\right)^2}}\right)}{k_m^\perp}, \tag{16a}$$

$$k_n[k_m^\perp] = \sqrt{\frac{\varepsilon_m - \left(k_m^\perp\right)^2}{1 - \varepsilon_m v_{\mathrm{F}}^2}}, \tag{16b}$$

where $k_m^\perp > 0$ [see Fig. 4(a)]. Interestingly, the $k_n[d]$ given in Eq. (16*a*) and (16*b*) are equal to the condition for the values of the wavevector at which the undisturbed odd waveguide modes cross the value $y = 1$. From Fig. 3 we can see that, in the region $y > 1$, the modes modified by the presence of graphene run between the even and odd modes of the pure dielectric waveguide.

From the previous reasoning it follows that in the region $y > 1$ only damped, even modes are allowed. Indeed, when graphene's pair-creation threshold is reached, a decay channel is introduced in the optical response of the system. Describing the slab-graphene-slab setup by an effective dielectric medium for the even modes and assuming that this effective medium $\varepsilon_{\mathrm{eff}} = \varepsilon + \varepsilon^{(1)}$ with $\varepsilon^{(1)} \ll \varepsilon$, we find that $\varepsilon^{(1)} \propto \alpha$ and thus

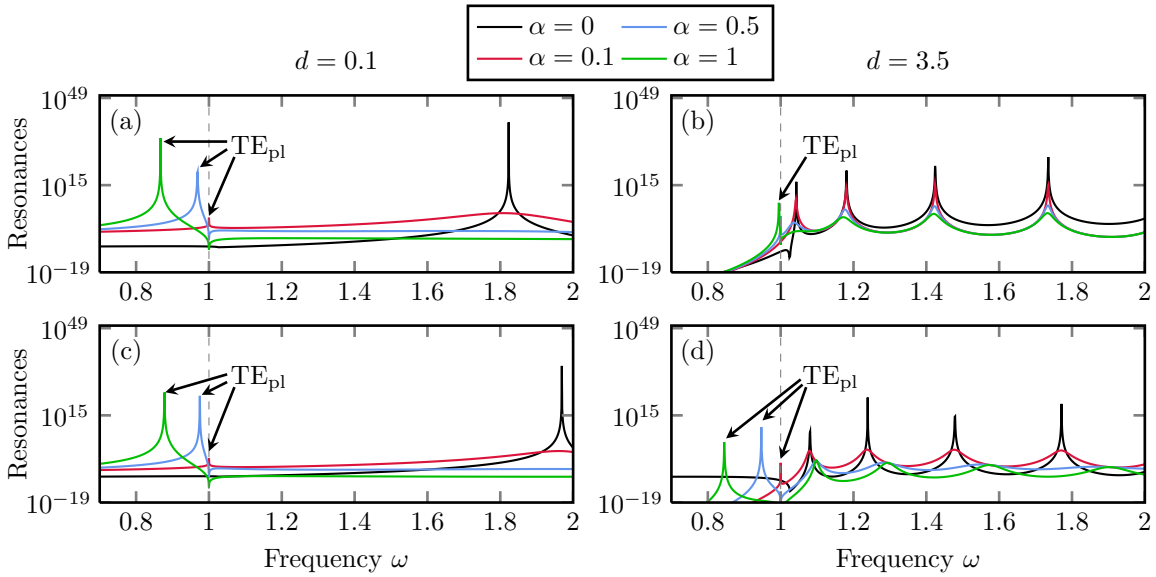


**Figure 5.** The Figure above shows the (damped) modes for $k_0 = 2.05$ and two different dielectric ($\varepsilon_m = 4$) slab thicknesses. The TE plasmonic resonance are denoted by $\mathrm{TE_{pl}}$ and can be found in the region $y < 1$. Panel (a,b): Solutions for graphene embedded between two slabs of thickness $d$. Depicted as resonance is the quantity (|l.h.s of Eq. (12)|$^{-10}$+l.h.s of Eq. (13)|$^{-10}$). $\alpha = 0$ shows only the even solutions of a waveguide without graphene of thickness $d' = 2d$ [Eq. (13) with $\alpha = 0$]. Only these even modes that are then altered when including graphene. Panel (c,d): Solutions for graphene embedded on top of a dielectric slab, where the plots show the quantity |l.h.s of Eq. (21)|$^{-10}$. $\alpha = 0$ shows the solution for a purely dielectric waveguide of thickness $d' = d$.

also the damping is proportional to $\alpha$. We remark that in Fig. 3 the even modes cannot be discerned since for large $\alpha$ the damping is very dominant. However, the modes and the corresponding damping become visible in Fig. 5(a,b) where we show cuts through Fig. 3 at $k_0 = 2.05$ while varying $\alpha$.

Returning to Eq. (15), we note that a second solution for $n = 0$ is possible if $2\kappa_0 + \alpha\Phi(y) > 0$. This corresponds to a mode with a dispersion relation always located below that of the vacuum TE-plasmon resonance (see Fig. 3). Curiously, this dispersion relation describes a field which is propagating along the direction orthogonal to the graphene layer for $0 < k < k_{\varepsilon_m}$ and evanescent for $k > k_{\varepsilon_m}$ [22, 23]. As before, the value of $k_{\varepsilon_m}$ depends on the systems parameters and can be found by solving

$$d = \lim_{\kappa_m \to 0} \left\{ \frac{1}{2\kappa_m} \ln \left[ \frac{(\kappa_0 - \kappa_m)\,(\alpha\Phi(\omega,k) - 2\kappa_m)}{(\kappa_0 + \kappa_m)\,(\alpha\Phi(\omega,k) + 2\kappa_m)} \right] \right\}$$
$$= -\frac{\alpha\Phi(y) + 2\kappa_0}{\alpha\kappa_0\Phi(y)}\,. \tag{17}$$

This leads to the parametric representation

$$k_{\varepsilon_m}[q] = \sqrt{\frac{\varepsilon_m}{1 - \varepsilon_m v_{\mathrm{F}}^2}}\tanh(q)\,, \tag{18a}$$

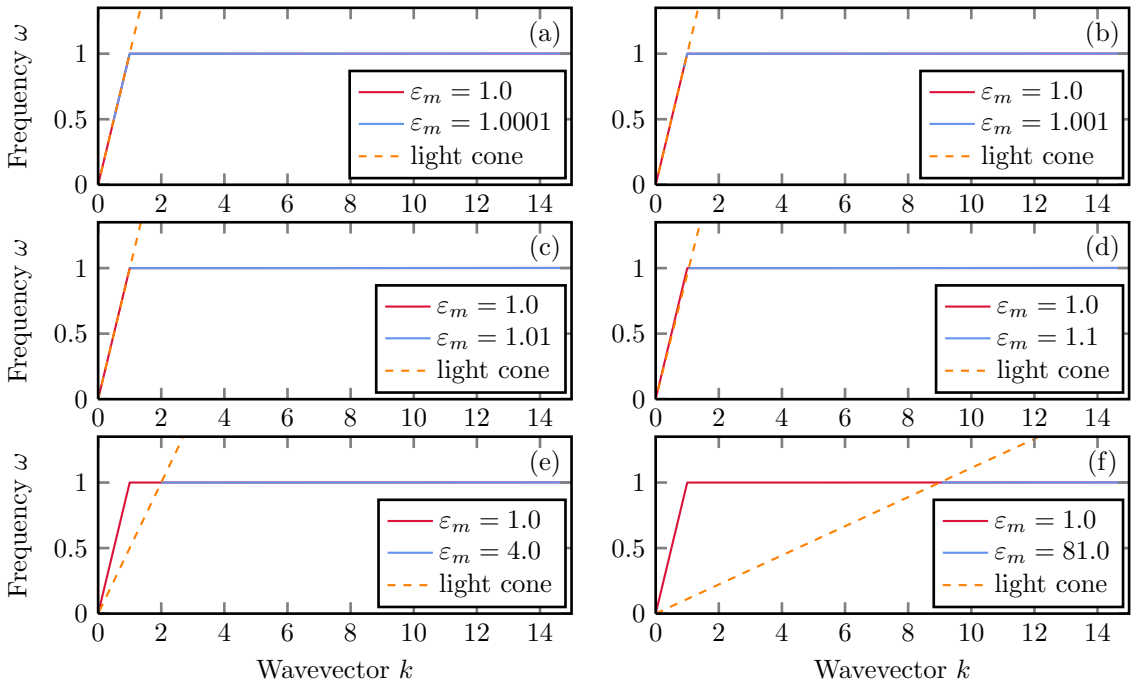


**Figure 6.** Dispersion relation of the TE surface plasmon in a graphene layer deposited on a bulk substrate with dielectric constant $\varepsilon_m$. In all subfigures, the substrate material's light cone is indicated by the dashed orange line. The red line represents the TE-plasmon dispersion relation for a graphene layer in vacuum.

$$d[q] \quad = -\frac{\alpha\Phi[\tanh(q)] + 2\sqrt{\frac{\varepsilon_m - 1}{1-\varepsilon_m v_{\mathrm{F}}^2}}\tanh(q)}{\alpha\sqrt{\frac{\varepsilon_m - 1}{1-\varepsilon_m v_{\mathrm{F}}^2}}\tanh(q)\Phi[\tanh(q)]} \tag{18b}$$

which we depict in Fig. 4(b). For $k \ll k_{\varepsilon_m}$, this dispersion relation starts along the vacuum light cone $\omega \lesssim k$, while in regions where the mode becomes evanescent ($k > k_{\varepsilon_m}$) the condition $2\kappa_m + \alpha\Phi(y) \leq 0$ must be satisfied. This implies that the dispersion relation of this mode lies above the TE-plasmon resonance of graphene embedded in an infinite material with dielectric permittivity $\varepsilon_m$ (see Fig. 3). Similar to this latter case, in the limit $k \to \infty$ the mode becomes independent of the material properties, approaching $\omega = \sqrt{1 + v_{\mathrm{F}}^2 k^2}$ from below.

The different physics associated with the two sets of modes also has an impact on their characteristics for increasing the slab's thickness. For $d \to \infty$ the number of waveguide modes increases but their dispersion relations remain confined in the region $\omega < k < \omega\sqrt{\varepsilon_m}$. The modes become denser and denser tending to the scattering waves of the infinite system (mathematically represented in the equations by a branch cut). In contrast, the singularity corresponding to the $n = 0$ solution remains isolated and actually approaches the dispersion relation given in Eqs. (9*a*) and (9*b*).

## 5. Graphene on a substrate

In most experimental setups graphene is deposited on dielectric substrates, i.e., in terms of our above analysis $\varepsilon_1 = 1$ and $\varepsilon_2 = \varepsilon_m$ with different thicknesses. In order to understand how the TE-plasmon resonances behave in this case, it is convenient to first consider the bulk limit case ($d_{1(2)} \to \infty$). Using $r_1(\kappa_{m,1} = \kappa_0) = 0$ and $r_2 \equiv r_m(d \to \infty) = \frac{\kappa_0 - \kappa_m}{\kappa_0 + \kappa_m}$, Eq. (8) leads to

$$r_m r_g - 1 = 0 \quad \Leftrightarrow \quad \alpha\Phi(y) + \kappa_0 + \kappa_m = 0 \; . \tag{19}$$

This has the parametric solution

$$k^2[y] = \frac{\omega[y]^2 - y^2}{v_{\rm F}^2} \tag{20a}$$

$$\omega^2[y] = \frac{4y^2 + v_{\rm F}^2\alpha^2\Phi(y)^2}{[2-(\varepsilon_m+1)v_{\rm F}^2]\left\{1+\sqrt{1-\left(\frac{(\varepsilon_m-1)v_{\rm F}}{2-(\varepsilon_m+1)v_{\rm F}^2}\right)^2\frac{4y^2+v_{\rm F}^2\alpha^2\Phi(y)^2}{\alpha^2\Phi(y)^2}}\right\}} \; , \tag{20b}$$

supplemented by the additional condition $\alpha^2\Phi(y)^2 \geqslant \kappa_0^2 + \kappa_m^2$. In Fig. 6, we display the corresponding dispersion relation and note that for $k > \omega\sqrt{\epsilon_m}$ it is rather similar to the dispersion relation for a gapped graphene layer in vacuum . Effectively, the material light cone cuts the dispersion relation for the TE-plasmon resonance and 'removes' the values for $k < \sqrt{\varepsilon_m/(1-\varepsilon_m v_{\rm F}^2)}$. For the parameters $\alpha = 137^{-1}$ and $v_{\rm F} = 300^{-1}$, already a substrate with a $\varepsilon_m > 1.1$ (see panel (d) in Fig.6) leads to dispersion relation that does not anymore depend on the properties of the dielectric. Despite this, a solution exists also for high values of the permittivity as long as $\varepsilon_m < v_{\rm F}^{-2}$.

More interesting is the case where the substrate has a finite thickness $d$. Similar to the two-slab configuration, the resonance condition

$$\begin{aligned} -\alpha\Phi(y)\left[(\kappa_0+\kappa_m)-(\kappa_0-\kappa_m)\mathrm{e}^{-2d\kappa_m}\right] \\ -(\kappa_0+\kappa_m)^2+(\kappa_0-\kappa_m)^2\mathrm{e}^{-2d\kappa_m} = 0\,, \end{aligned} \tag{21}$$

can be recast as

$$d = \frac{1}{2\kappa_m}\ln\left(\frac{(\kappa_0-\kappa_m)\left(\alpha\Phi(y)+\kappa_0-\kappa_m\right)}{(\kappa_0+\kappa_m)\left(\alpha\Phi(y)+\kappa_0+\kappa_m\right)}\right). \tag{22}$$

Due to the asymmetry of this setup, opposite to Eq. (13) all waveguide modes are altered by the presence of graphene. The analysis of Eq. (22) proceeds along lines that are similar to those discussed in the previous section. Also in this case, two sets of modes are possible (see Fig. 7). We obtain a TE-plasmon resonance which exists for all $k$, crossing the material light cone for $k = k_{\varepsilon_m}$. In this latter case the $k_{\varepsilon_m}$ has the following dependence on the substrate thickness

$$k_{\varepsilon_m}[q] = \sqrt{\frac{\varepsilon_m}{1-\varepsilon_m v_{\rm F}^2}}\tanh(q)\,, \tag{23a}$$

$$d[q] \quad = -\frac{\alpha\Phi[\tanh(q)] + 2\sqrt{\frac{\varepsilon_m-1}{1-\varepsilon_m v_{\rm F}^2}}\tanh(q)}{\left\{\alpha\Phi[\tanh(q)] + \sqrt{\frac{\varepsilon_m-1}{1-\varepsilon_m v_{\rm F}^2}}\tanh(q)\right\}\sqrt{\frac{\varepsilon_m-1}{1-\varepsilon_m v_{\rm F}^2}}\tanh(q)}. \tag{23b}$$

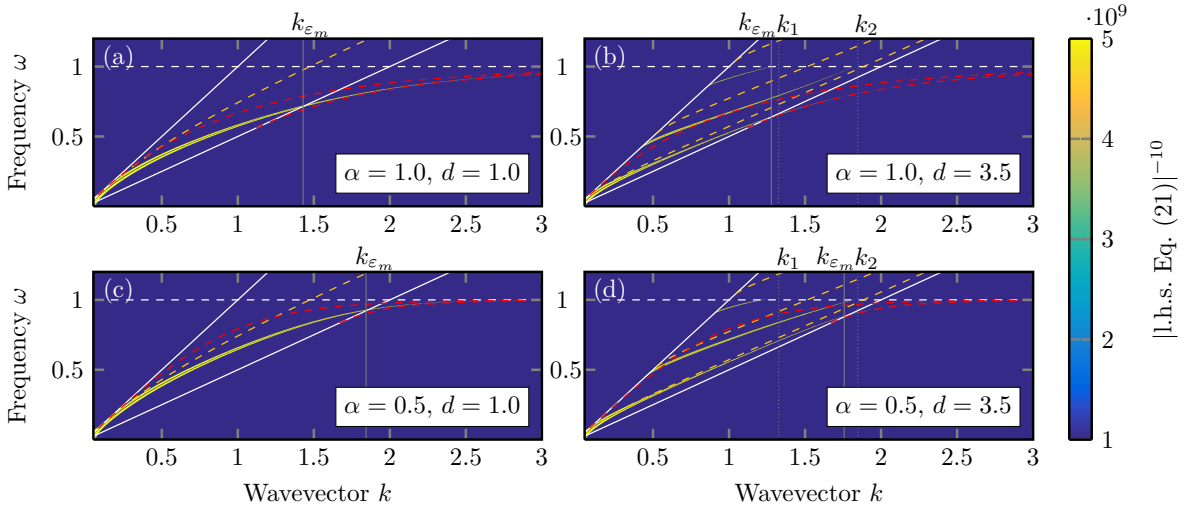


**Figure 7.** TE-plasmon resonances for a graphene layer on a dielectric substrate with finite thickness. The slab's waveguide modes are indicated by the dashed orange lines. A TE-plasmon resonance that crosses the material's light cone is discernible. The red dashed lines represent the solution of the TE-plasmon mode for a graphene layer in vacuum (upper row) and a graphene layer deposited on an infinitely extended substrate with dielectric function $\varepsilon_m$ (lower row). The remaining parameters are the same as in Fig. 3.

In Fig. 4, we represent this solution by dashed lines. The dispersion relation describing this resonance lies between the symmetric vacuum expression given in Eqs. (9$a$) and (9$b$) and the asymmetric bulk dispersion relation of Eqs. (20$a$) and (20$b$) (red dashed lines in Fig. 7), rapidly approaching this last curve for $k > k_{\varepsilon_m}$. For $k \to 0$ the dispersion relation of the TE-plasmon follows the vacuum light cone and shows the same asymptotic behavior as the lowest-frequency solution of

$$(\kappa_0 + \kappa_m)^2 - (\kappa_0 - \kappa_m)^2 \mathrm{e}^{-2d\kappa_m} = 0\,, \tag{24}$$

the solutions of which represent ordinary waveguiding modes in simple dielectric slabs. In Figs. 7, we observe that indeed the TE-plasmon dispersion relation approaches the orange dashed line that describes the zeroth waveguiding mode of a single dielectric slab.

As in the double-slab configuration discussed in the previous section, we find here that undamped waveguide modes only exist in the regions $\omega < k < \omega\sqrt{\varepsilon_m}$ and $y \leq 1$. Due to pair-creation, analogously to the slab-graphene-slab case, damped waveguide modes exist for $y > 1$ [cf. Fig. 5(c,d)]. Here, the damping also increases with increasing $\alpha$. Once again, the graphene layer imposes a cutoff on the real solutions of Eq. (24) and the undamped modes end on $y = 1$ for values of $k_n$ given as in the symmetric two-slab case by Eqs. (16$a$) and (16$b$).

## 6. Conclusions

We have investigated the electromagnetic characteristics of different graphene-dielectric structures and have demonstrated that, when a gap appears in the graphene's band structure, TE-plasmon resonances exist for large values of the dielectric permittivity. Depending on the actual realization, the characteristics of the corresponding dispersion relations are quite different, in certain cases describing waves that change their nature from propagating to evanescent as a function of the wavevector. When graphene is deposited on a bulk substrate only the evanescent part of the dispersion relation remains as an isolated singularity, while the propagating part merges in the continuum of scattering states in the semi-infinte medium. We have further shown, that when graphene is in contact with one or two slabs of finite thickness, the slab's real waveguiding modes exhibit a cutoff frequency whose value corresponds to the energy threshold for pair-creation in graphene (single particle excitation threshold). Modes with frequency above this cutoff are damped since the pair-creation constitutes a loss channel. Quantum properties of graphene, specifically the pair-creation, thus affect both, the TE-plasmon properties and the waveguiding modes introducing additional losses in the electromagnetic response. Because these effects are related to the existence of a band gap, they do not appear in recent studies that address waveguiding modes for gapless graphene-dielectric structures [24] (see also very recent studies for metal-graphene setups [25, 26, 27, 28, 29]). If we were to include additional loss channels into the description of graphene such as a finite relaxation rate for the carriers in graphene, these losses would increase.

The above results are of interest for several experimentally relevant scenarios such as atom-chip systems. In these systems, a cloud of cold or ultra-cold atoms are magnetically trapped near surfaces [30, 31]. As TE-polarized fields have a large magnetic component, the TE-plasmons and all further TE waveguiding modes associated with graphene-dielectric structures may profoundly affect the dynamics of magnetic emitters as they provide additional decay channels. The thorough understanding of these modes is thus key to the correct description and characterization of the decay dynamics of such emitters. Finally, the opportunity to damp and thus filter certain waveguiding modes by including a graphene layer with tunable band gap [4] may open novel paths for technological applications, notably in the area of nano-photonic systems.

## 7. Acknowledgements

We acknowledge support by the Deutsche Forschungsgemeinschaft (DFG) through the Collaborative Research Center (CRC) 951 "Hybrid Inoganic/Organic Systems for Optoelectronics (HIOS)" within project B10. FI further acknowledges financial support from the EU through the Career Integration Grant (CIG) No. 631571 and support by the DFG through the DIP program (FO 703/2-1).

[1] McCann E 2012 Electronic properties of monolayer and bilayer graphene *Graphene Nanoelectronics* NanoScience and Technology (Berlin Heidelberg: Springer) pp 237–275
[2] Giovannetti G, Khomyakov P A, Brocks G, Kelly P J and van den Brink J 2007 *Phys. Rev. B* **76** 073103
[3] Zhou S, Gweon G H, Fedorov A, First P, De Heer W, Lee D H, Guinea F, Neto A C and Lanzara A 2007 *Nat. Mater.* **6** 770
[4] Jung J, DaSilva A M, MacDonald A H and Adam S 2015 *Nat. Commun.* **6** 6308
[5] Christensen J, Manjavacas A, Thongrattanasiri S, Koppens F H and Garciía de Abajo F J 2011 *ACS Nano* **6** 431
[6] Christensen T, Wang W, Jauho A P, Wubs M and Mortensen N A 2014 *Phys. Rev. B* **90** 241414
[7] Alkorre H, Shkerdin G, Stiens J and Vounckx R 2015 *J. Opt.* **17** 045003
[8] Jadidi M M, Sushkov A, Myers-Ward R L, Boyd A, Daniels K, Gaskill D K, Fuhrer M S, Drew H D and Murphy T E 2015 *Nano Lett.* **15** 7099
[9] Kumar A, Nemilentsau A, Fung K H, Hanson G, Fang N X and Low T 2015 *arXiv preprint arXiv:1509.00790*
[10] Cai X, Sushkov A B, Jadidi M M, Nyakiti L O, Myers-Ward R L, Gaskill D K, Murphy T E, Fuhrer M S and Drew H D 2015 *Nano Lett.* **15** 4295
[11] Mikhailov S and Ziegler K 2007 *Phys. Rev. Lett.* **99** 016803
[12] Kotov O, Kol'chenko M and Lozovik Y E 2013 *Opt. Expr.* **21** 13533–13546
[13] Stauber T 2014 *J. Phys. - Condens. Mat.* **26** 123201
[14] Gusynin V, Sharapov S and Carbotte J 2007 *Int. J. Mod. Phys. B* **21** 4611
[15] Fialkovsky I V, Marachevsky V N and Vassilevich D V 2011 *Phys. Rev. B* **84** 035446
[16] Chaichian M, Klimchitskaya G, Mostepanenko V and Tureanu A 2012 *Phys. Rev. A* **86** 012515
[17] Bordag M and Pirozhenko I 2014 *Phys. Rev. B* **89** 035421
[18] Bordag M and Pirozhenko I 2015 *Phys. Rev. D* **91** 085038
[19] Klimchitskaya G, Mohideen U and Mostepanenko V 2014 *Phys. Rev. B* **89** 115419
[20] Klimchitskaya G, Korikov C and Petrov V 2015 *Phys. Rev. B* **92** 125419
[21] Saleh B E A and Teich M C 2007 *Fundamentals of Photonics* 2nd ed (Hoboken, N.J.: Wiley)
[22] Intravaia F and Lambrecht A 2005 *Phys. Rev. Lett.* **94** 110404
[23] Intravaia F, Henkel C and Lambrecht A 2007 *Phys. Rev. A* **76** 033820
[24] Hanson G W 2008 *J. Appl. Phys.* **104** 084314
[25] Khromova I, Andryieuski A and Lavrinenko A 2014 *Laser Photon. Rev.* **8** 916
[26] Ralević U, Isić G, Vasić B and Gajić R 2014 *J. Phys. D: Appl. Phys.* **47** 335101
[27] Luo X, Zhai X, Wang L and Lin Q 2015 *Plasmonics* 1
[28] Shkerdin G, Alkorre H, Stiens J and Vounckx R 2015 *J. Opt.* **17** 055006
[29] Degli-Eredi I, Sipe J and Vermeulen N 2015 *Opt. Lett.* **40** 2076
[30] Fortágh J and Zimmermann C 2007 *Rev. Mod. Phys.* **79** 235
[31] Folman R, Krüger P, Schmiedmayer J, Denschlag J and Henkel C 2002 *Adv. At. Mol. Opt. Phys.* **48** 263